ASSSP12 University of Warwick 2-7 Sep 2012

Sun Observation

Erwin Verwichte

Overview of aspects of solar observation focused mainly on EUV imaging of the solar corona.

Centre for Fusion, Space and Astrophysics
THE UNIVERSITY OF WARWICK

The ‘Carrington’ Experience

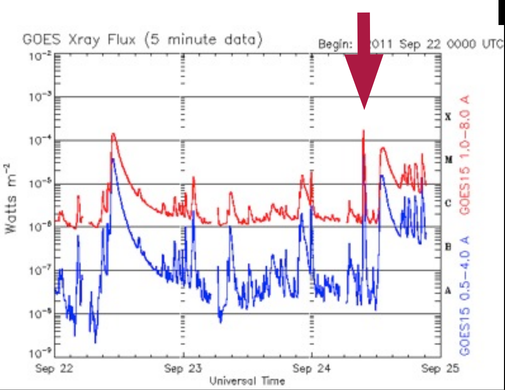

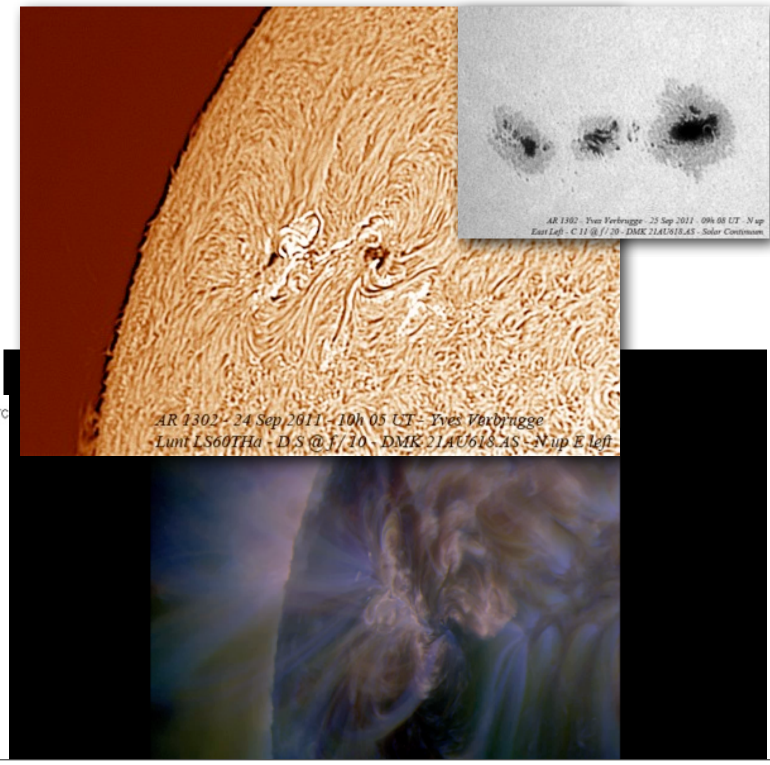

Observational Scales

With current instruments we resolve dynamics on macroscopic scales, where magnetohydrodynamics is applicable.

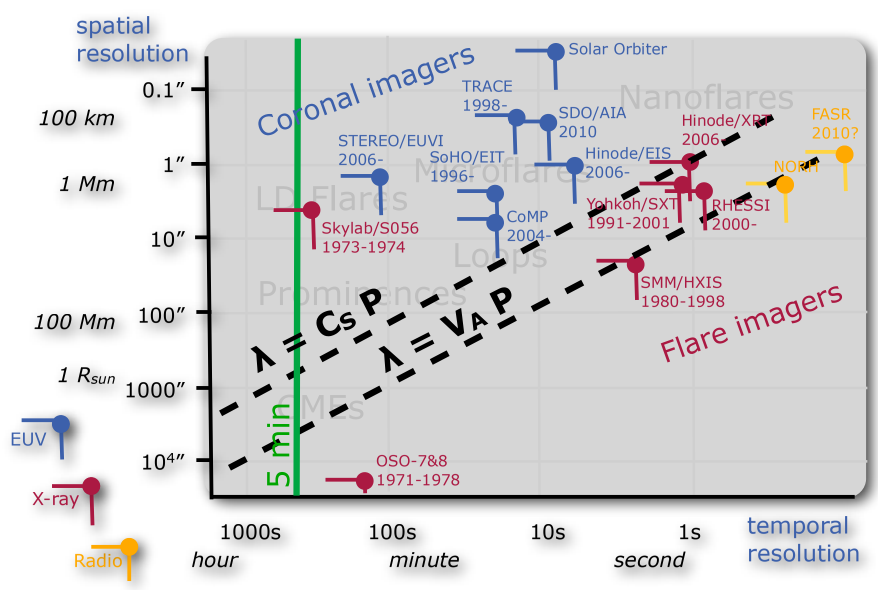

C_S: speed of sound, V_A: Alfvén speed

The Solar atmosphere

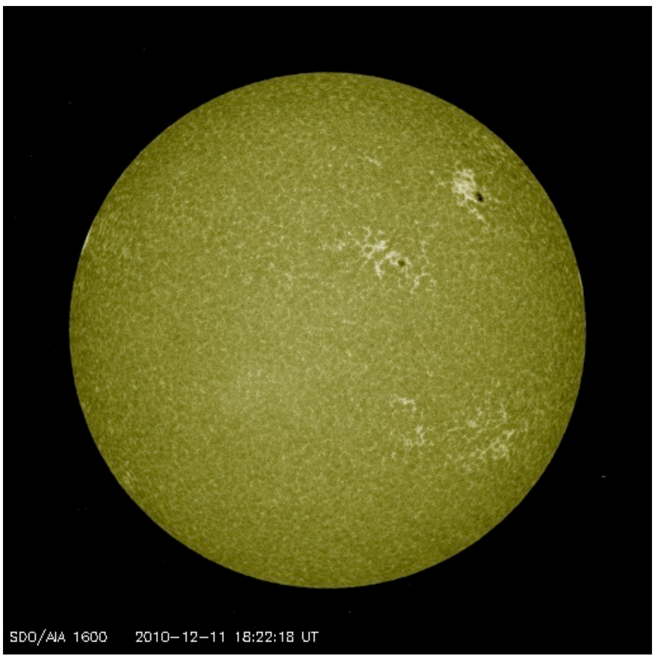

The Sun's appearance changes throughout the atmosphere

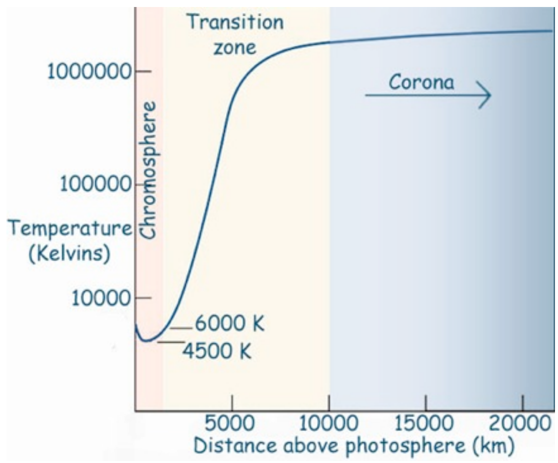

The Solar atmosphere

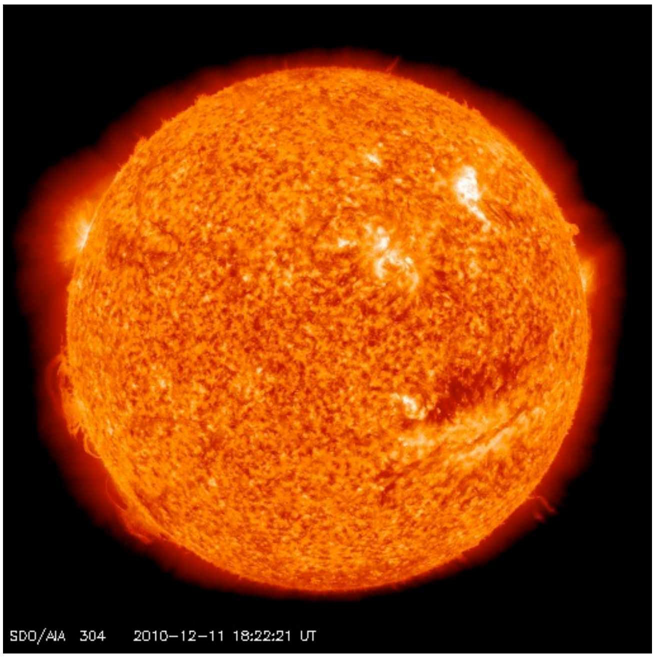

The Sun's appearance changes throughout the atmosphere

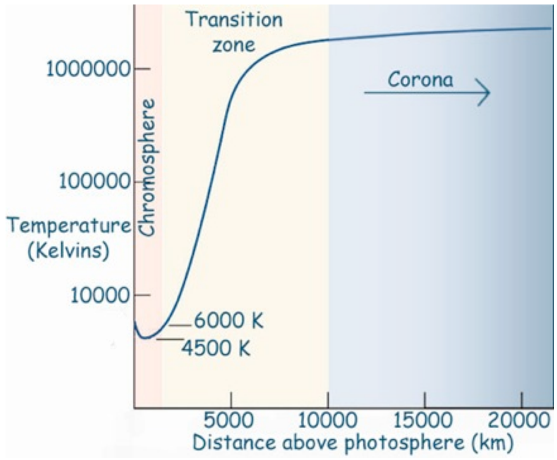

The Solar atmosphere

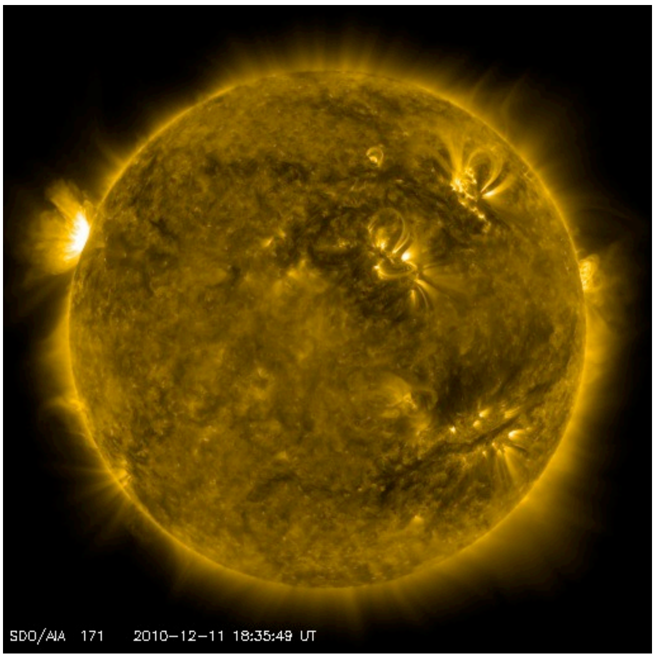

The Sun's appearance changes throughout the atmosphere

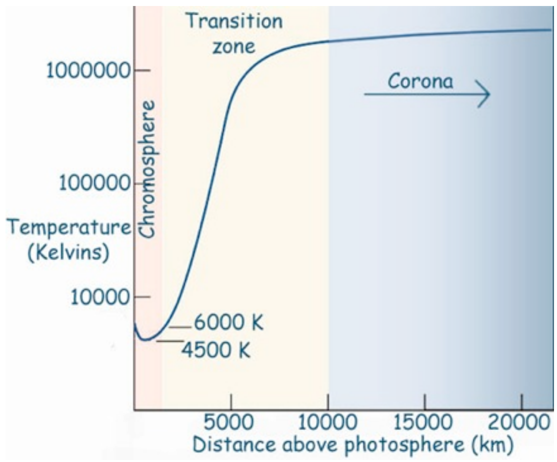

The Solar atmosphere

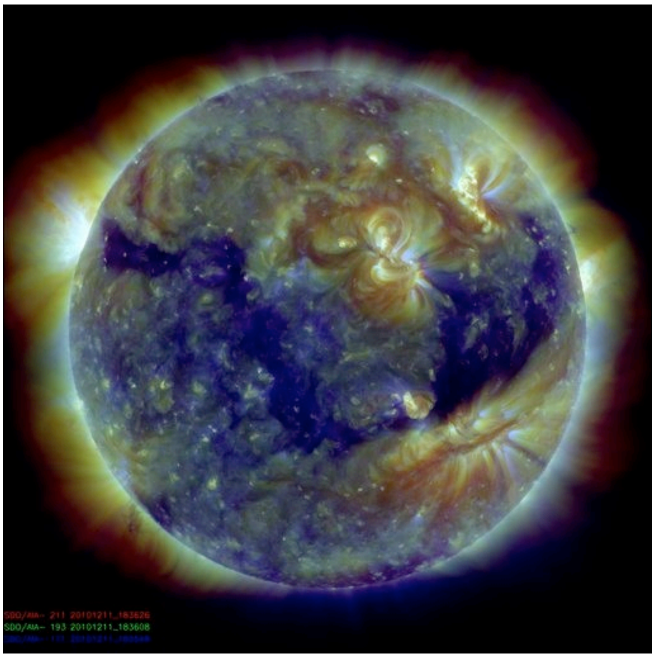

The Sun's appearance changes throughout the atmosphere

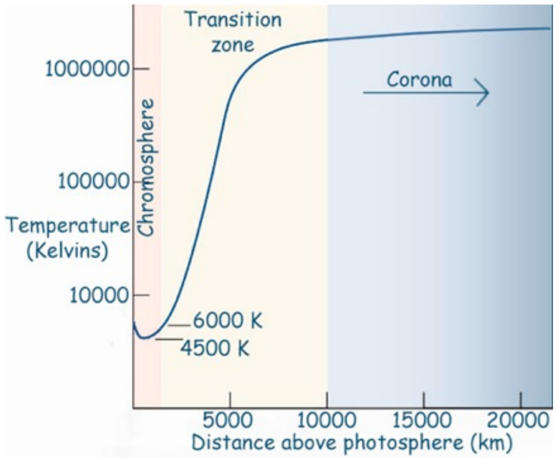

3
Erwin Verwichte - Sun Observation - ASSSP12
The Solar atmosphere

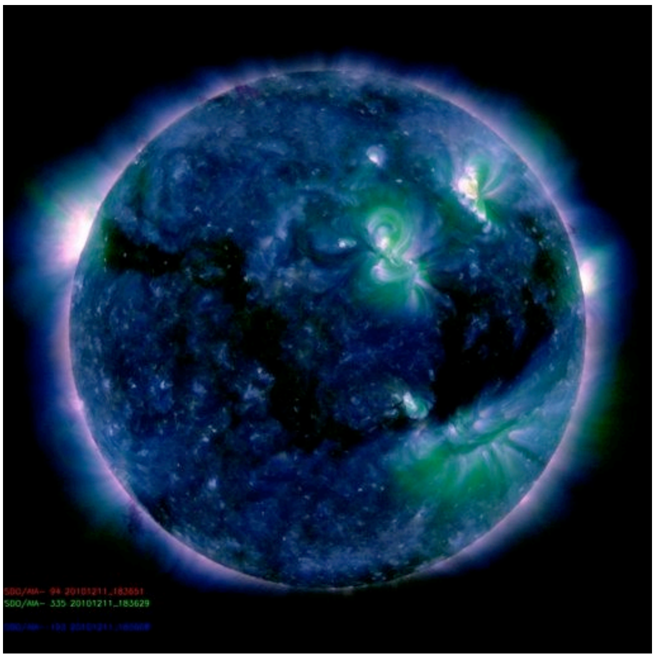

The Sun's appearance changes throughout the atmosphere

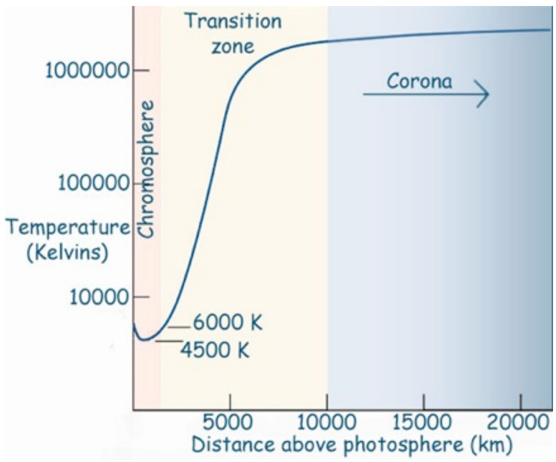

The Solar atmosphere

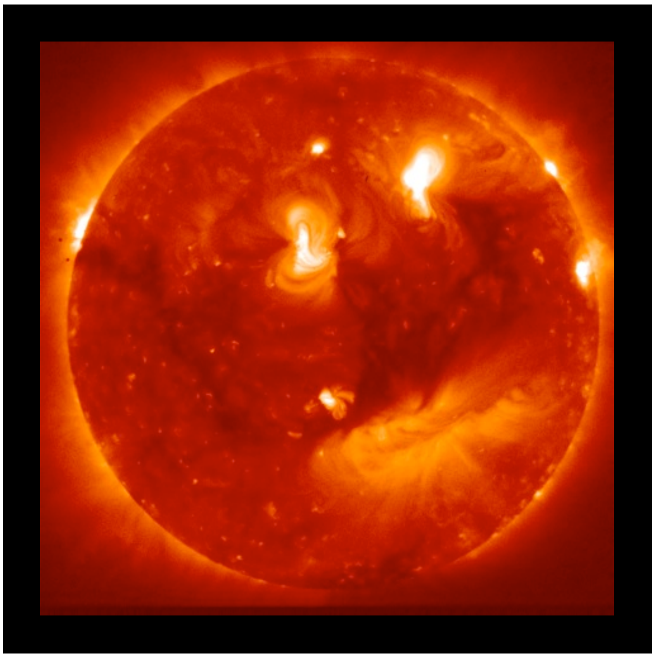

The Sun's appearance changes throughout the atmosphere

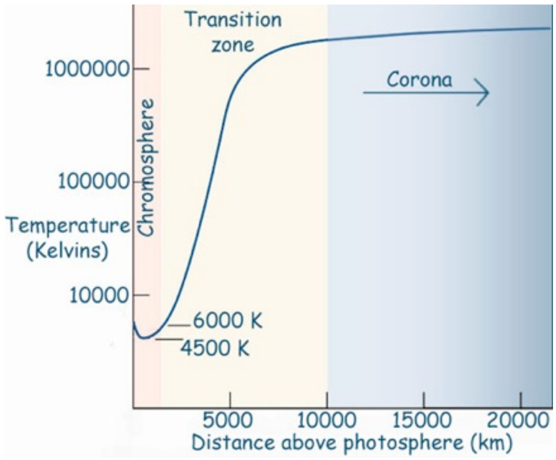

4

Solar spectrum

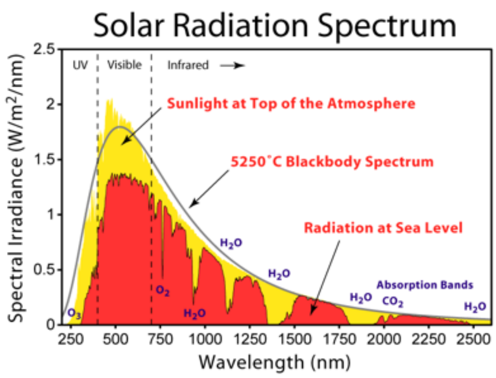

The largest part of solar radiation comes from the photosphere, which can be modeled as a black-body radiator visible in the visible, UV and IR, with elements providing absorption lines,

The corona is optically thin, filled with rarified plasma at millions of degrees Kelvin and its thermal part emits through line-emission from minority species excited by collisions. This gives rise to emission line spectra, visible in the EUV and X-ray.

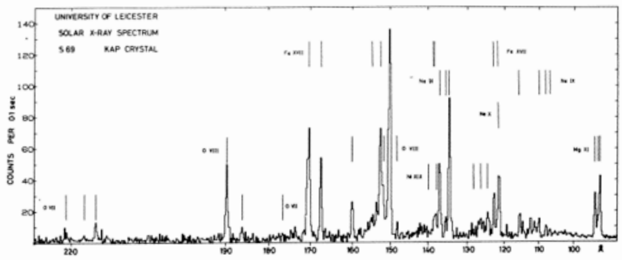

THE SOLAR X-RAY SPECTRUM 365

Figure 3 X-ray spectrum of a solar active region obtained on 6 December 1970 by a collimated Bragg crystal spectrometer flown by the University of Leicester. These uncorrected data do not represent true relative line intensities but clearly illustrate the dominance of line emission in this spectral region. Identity of the parent ions for the stronger lines are indicated. (Courtesy of J. H. Parkinson, University College, London.)

Culhane & Acton (1974)

Earth atmosphere is a barrier to observe the corona?

There are two windows to observe space from the ground: visible and radio

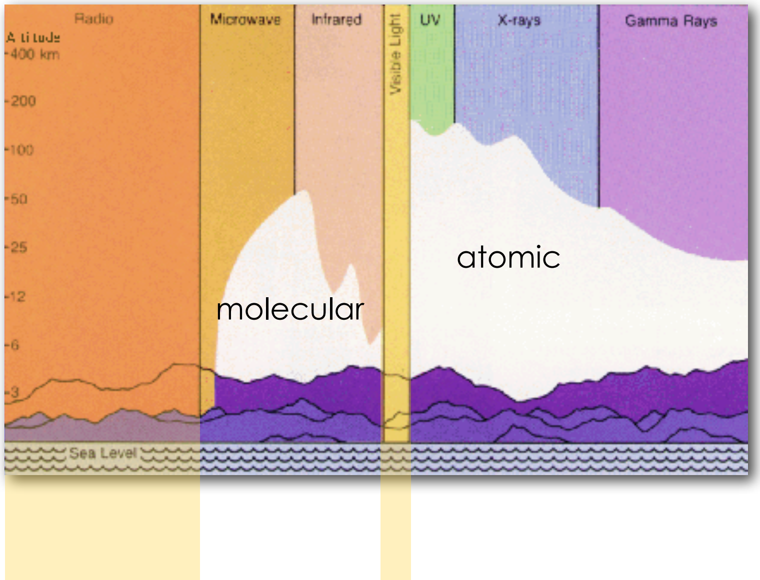

Natural and unnatural coronagraphs

The corona can be seen in the visible light because its electrons (K-corona) and dust (F-corona) scatter light from the photosphere. *Intensity is proportional to density (info on structuring), scattering has no temperature info.*

by the moon

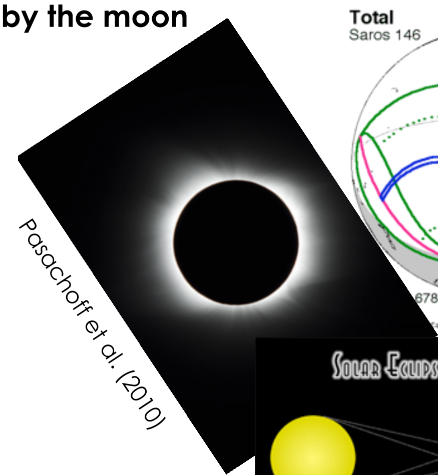

Pasachoff et al. (2010)

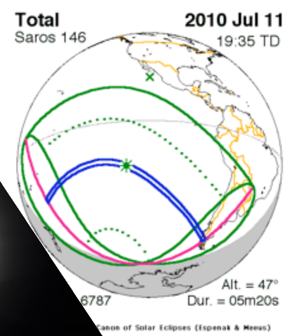

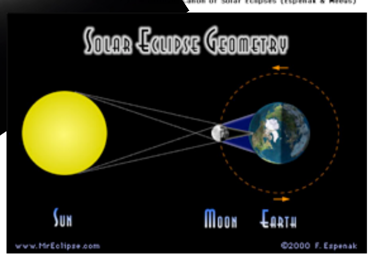

by an artificial obstruction

Invented by Bernard Lyot in 1939

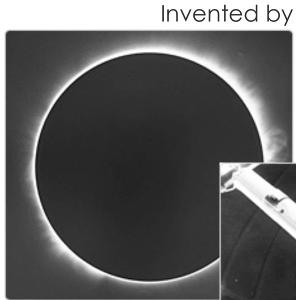

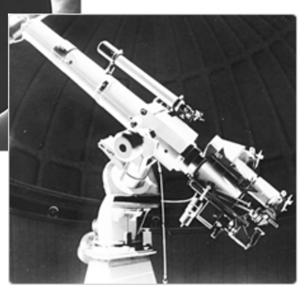

National Astronomical Observatory of Japan

Downsides: at mercy of orbital mechanics of the Moon and at mercy of the Earth's atmospheric conditions.

Natural and unnatural coronagraphs

There are ‘forbidden’ emission lines in the visible spectrum that are sensitive to coronal temperatures that offer more, e.g. Fe XIII at 1074.7 nm!

<u>Example:</u> Polarimeter which measures the polarization of the light with a coronagraph at several wavelengths around the emission line.

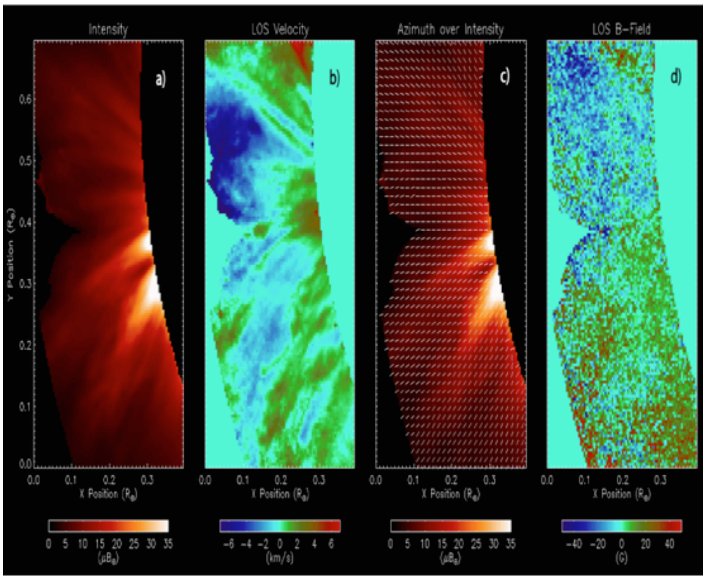

CoMP (Tomczyk et al. 2008)

Ground-measurements are flexible and can be sensitive and high time-cadence, but again you are at the mercy of the Earth’s atmosphere!

Stokes parameters

Stokes parameters describe the coherence and polarization of light.
We measure the light as a vector in the plane of the sky using polarizing filters.

I = $|E_x|^2 + |E_y|^2$ Total intensity (coherent + incoherent)
Q = $|E_x|^2 - |E_y|^2$ Horizontal-vertical linear polarization balance
U = $|E_a|^2 - |E_b|^2$ 45 degrees linear polarization balance
V = $|E_L|^2 - |E_R|^2$ Left-right circular polarization balance
also
P = $[\mathbf{Q}^2 + \mathbf{U}^2]^{1/2}$ Polarization

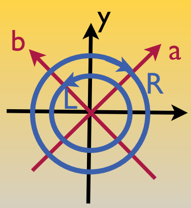

The Stokes parameters contain information about the *magnetic field*:

- Line-of-sight magnetic field from **V** (Zeeman, tricky in corona as **V/I** < 0.001)
- Plane-of-sky magnetic field direction from **Q** and **U** (resonance scattering)

$$V \propto B \cos\theta_B \left(\frac{\mathrm{d}I}{\mathrm{d}\omega}\right)$$

$$P \propto \sin^2(\theta_B)\, I$$

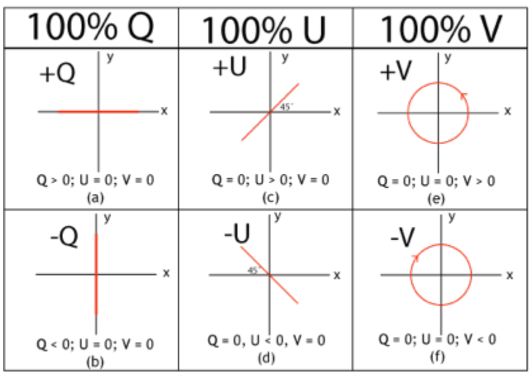

Imaging in the EUV

An EUV imager takes images of the Sun through a broadband wavelength filter in which one (or several) dominant EUV emission line(s) are present.

You cannot use refraction (lenses) in the EUV domain because matter absorbs this light. EUV telescopes thus need to use reflection (mirrors).

One traditional method is using diffraction grating (e.g. Skylab, MOSES rocket).

Skylab overlappograph

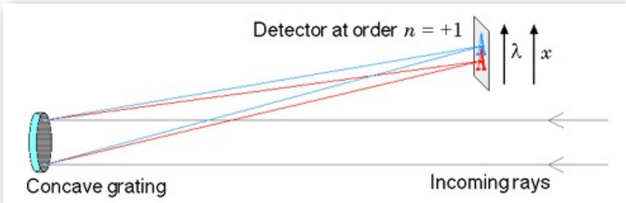

Extreme-ultraviolet Imaging Telescope (EIT)

A first instrument that uses normal incidence (reflection of a mirror) is the **Extreme-ultraviolet Imaging Telescope** (EIT) on board SoHO.

EIT

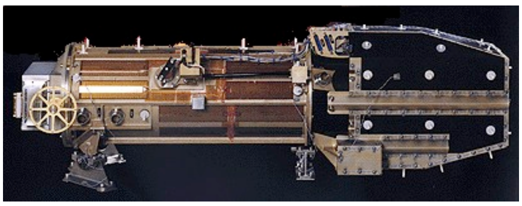

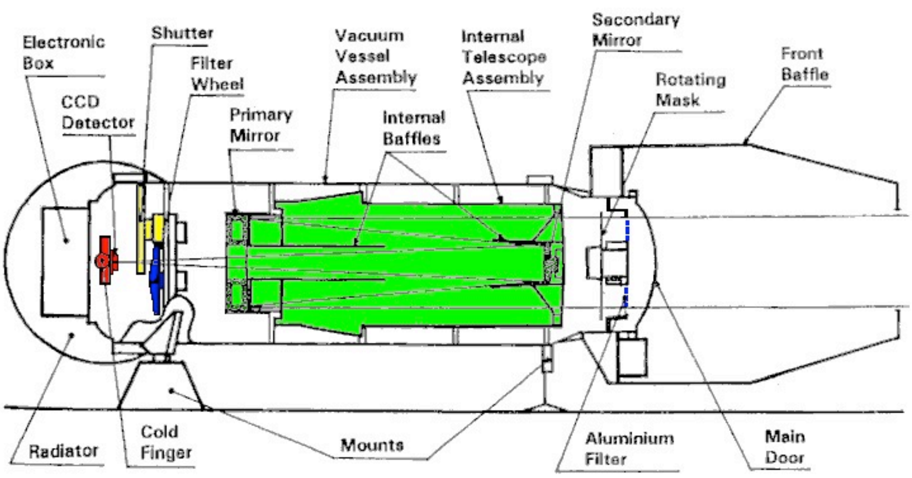

Extreme-ultraviolet Imaging Telescope (EIT)

Al-filters block out the visible part of the solar spectrum (just as eclipse glasses would). They are mounted on two filter support grids.

A sector wheel allows to select one of the four quadrants of the optics.

The optics are a Ritchey-Chretien design (a bit like a Cassegrain). They are multi-layer coated with Mo and Si. Each quadrant is different, with a different EUV wavelength window.

The shutter lets the CCD see or not see the EUV light.

The filter wheel allows to add some additional Al-filtering.

A stray-light filter eliminates any reflections off instrument parts.

CCD is 1024x1024 back-illuminated.

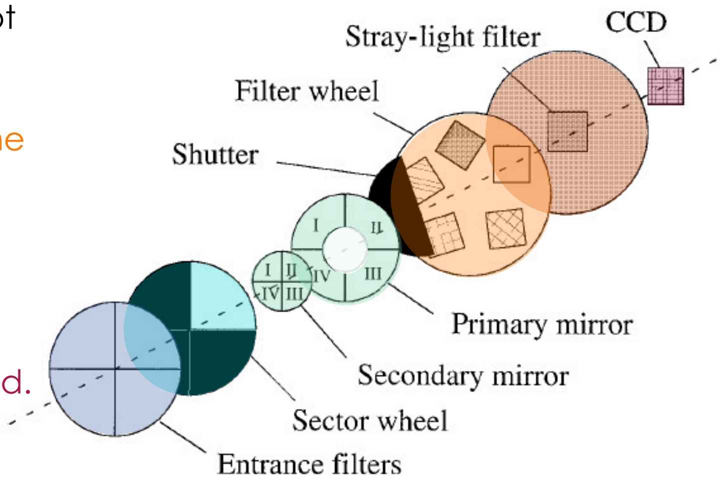

Extreme-ultraviolet Imaging Telescope (EIT)

The throughput (transfer function) of the telescope:

$$I(x,y) = \int_0^\infty A_{\mathrm{eff,i}}(\lambda)\, G(\lambda)\, F(x,y) \int_{(x,y)} P(\lambda,\theta,n_e,T) * \mathrm{PSF}(\theta)\mathrm{d}\theta\,\mathrm{d}\lambda$$

To compare with other instruments we use the **Effective Area**:

$$A_{\mathrm{eff}}(\lambda) = A\, T_{\mathrm{EF}}(\lambda)\, R_{\mathrm{PM}}(\lambda)\, R_{\mathrm{SM}}(\lambda)\, T_{\mathrm{FW}}(\lambda)\, T_{\mathrm{SL}}(\lambda)\, \epsilon(\lambda)\, D(\lambda,t)$$

A: open aperture area [cm^2] = 11.97
$T_{EF}(\lambda)$: Entrance Filter transmissivity [1]
$R_{PM}(\lambda)$: Primary Mirror reflectivity [1]
$R_{SM}(\lambda)$: Secondary Mirror reflectivity [1]
$T_{FW}(\lambda)$: Filter Wheel transmissivity [1]
$T_{SL}(\lambda)$: Stray-Light Filter transmissivity [1]
$\varepsilon(\lambda)$: CCD quantum efficiency [1]
$D(\lambda,t)$: Degradation over time [1]

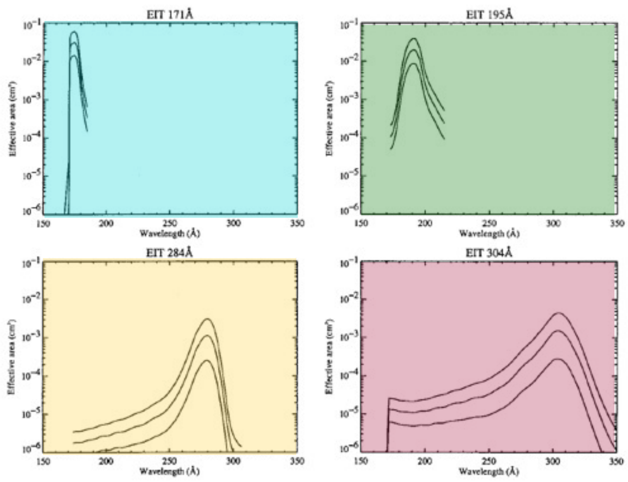

(Dere et al. 2000).

G is the gain of the CCD-camera in DN (Digital Number) per photon. In other words, how much image value is a photon worth?

$$G(\lambda) = \frac{12398}{3.65\lambda}\,g$$

with *g* how many electrons makes one DN.

F(x,y) is the CCD flat-field. Not all pixels are of identical quality.

Also, integration over the space-angle θ for the pixel can be written as

$$\int_{(x,y)} \mathrm{d}\theta = \left(\frac{a_{\rm pix}}{f}\right)^2$$

where a_{pix} is the CCD pixel area and *f* the telescope focus, which is a function of wavelength

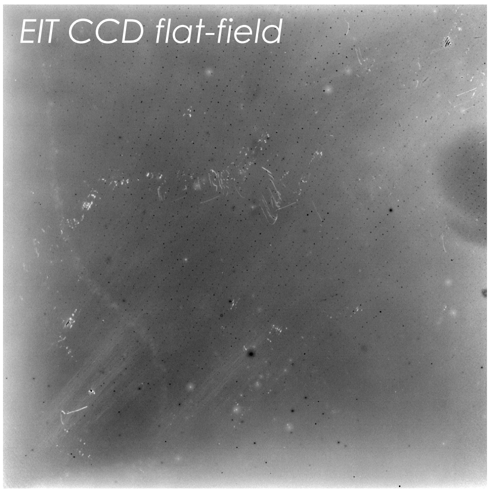

The **point-spread function** PFS is the shape of a point source at the CCD after it passed through all the optics. This includes entrance and other filter diffraction (remember grid!) and the two mirrors

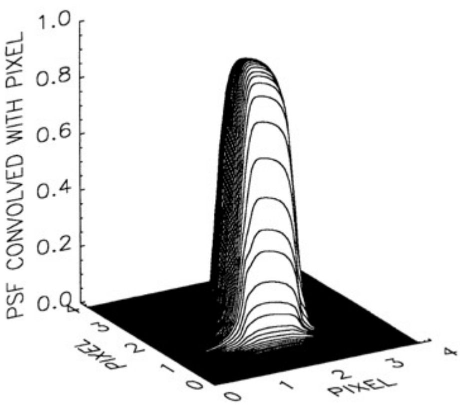

core PSF convolved with a pixel for EIT 304Å bandpass

AIA/SDO full PSF (Grigis et al 2012)

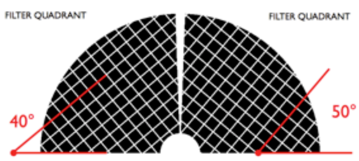

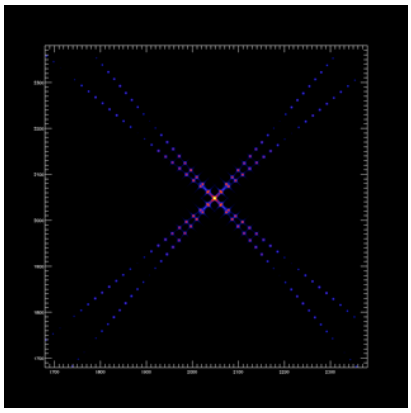

Extreme-ultraviolet Imaging Telescope (EIT)

Also, the incident solar flux [photons $cm^{-2}\,s^{-1}\,sr^{-1}\,Å^{-1}$] may be split into the atomic emission line details and the emissivity of the plasma:

$$P(\lambda, n_e, T) = \int_0^\infty \mathcal{G}(\lambda, n_e, T)\,\mathrm{DEM}(T)\,\mathrm{d}T$$

where G contains the atomic information of all emission lines (and free). This function is usually much stronger temperature than density dependent.

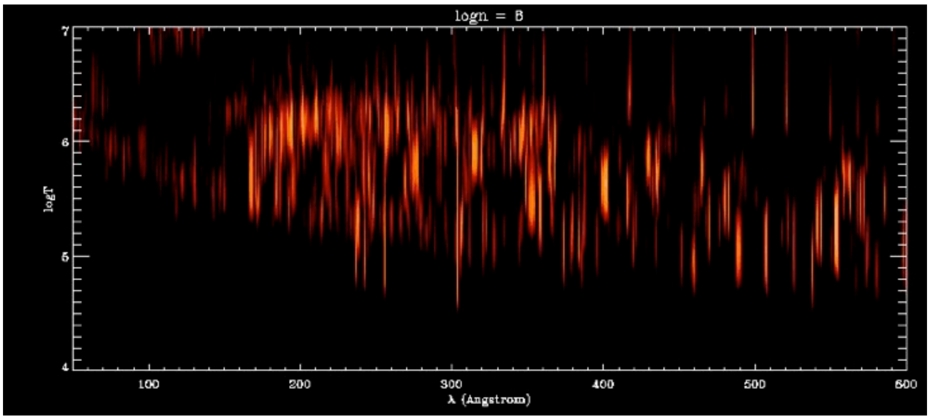

Created using CHIANTI

Extreme-ultraviolet Imaging Telescope (EIT)

First, we define the emission EM to be the line-of-sight integration emissivity $n_e\, n_H$ (we assume resonance emission line excited by collisions):

$$\mathrm{EM} = \int_{\mathrm{LOS}} n_e(T,z)\, n_H(T,z)\,\mathrm{d}z$$

The Differential Emission Measure (DEM) is defined as the distribution of emissivity ($n_e\, n_H$) in the line-of-sight as a function of temperature(linear version).

$$\mathrm{DEM} = \frac{\mathrm{dEM}}{\mathrm{d}T} = n_e n_H \frac{\mathrm{d}z}{\mathrm{d}T} \quad \mathrm{or} \quad \mathrm{DEM} = \int_T^{T+\mathrm{d}T} n_e n_H \left(\frac{\mathrm{d}z}{\mathrm{d}T}\right)\mathrm{d}T$$

and

$$\mathrm{EM} = \int_0^\infty \mathrm{DEM}(T)\,\mathrm{d}T$$

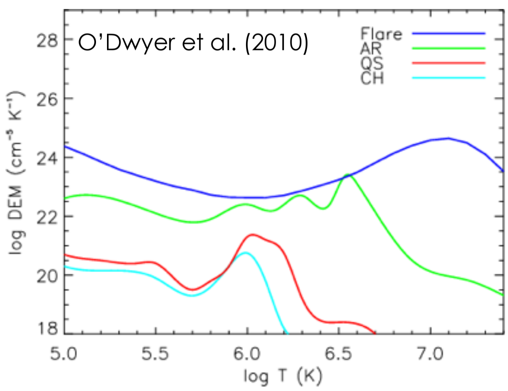

Extreme-ultraviolet Imaging Telescope (EIT)

Putting all together, we can describe the instrument's response in terms of temperature bandpasses *H(T)*:

$$I = \int_0^\infty H(T)\,\mathrm{DEM}(T)\,\mathrm{d}T \qquad H(T) = \int_0^\infty A_{\mathrm{eff},i}(\lambda)\,G(\lambda)\left(\frac{a_{\mathrm{pix}}}{f}\right)^2 \mathcal{G}(\lambda, n_e(T), T)\,\mathrm{d}\lambda$$

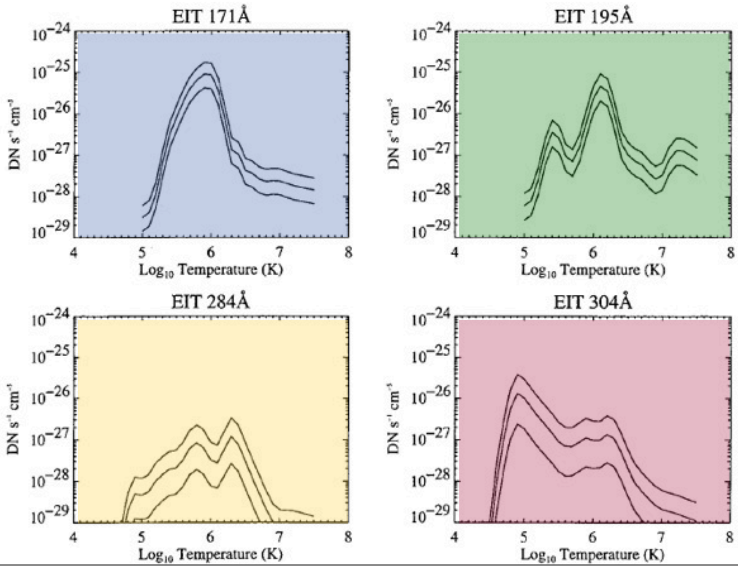

Because multiple emission lines contribute to H(T), its shape can be multi-peaked.

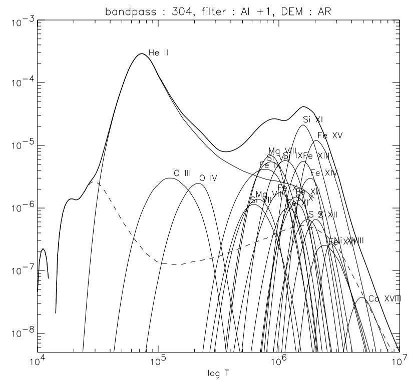

Extreme-ultraviolet Imaging Telescope (EIT)

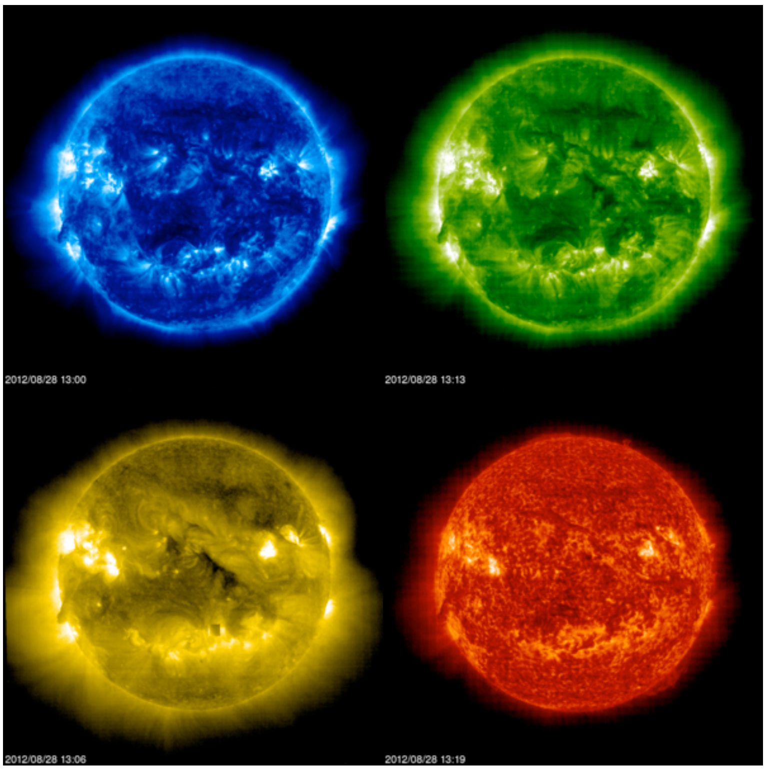

Extreme-ultraviolet Imaging Telescope (EIT)

Example of degradation of the CCD. Because the entrance filter grid throws a shadow onto the CCD, those pixels in the shadow have seen less total light and have less degraded. Hence, their gain is higher. In images we see the grid as a bright feature!

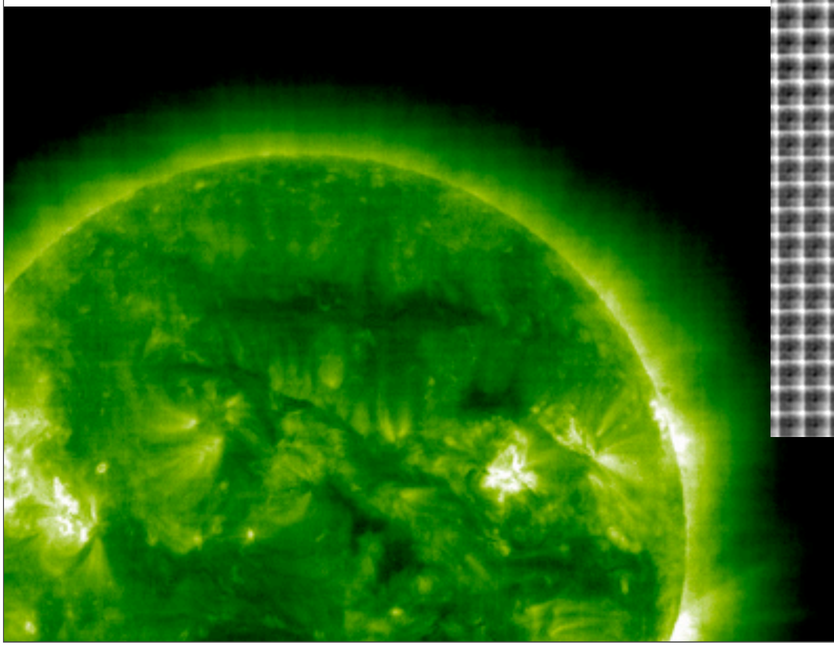

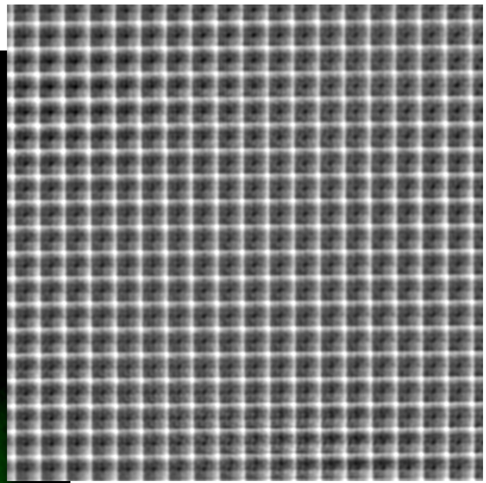

Temperature bandpass ratio

We can take the ratio of two bandpasses and in a certain interval of temperature, where the ratio is monotonic and near the peak responses of the two bandpasses, we can estimate the temperature crudely.

Assume the coronal plasma is isothermal, i.e. $DEM(T) = EM_0\, \delta(T-T_0)$. Then,

$$\left.\begin{array}{l} I_1 = H_1(T_0)\, EM_0 \\ I_2 = H_2(T_0)\, EM_0 \end{array}\right\} \Rightarrow \frac{I_1}{I_2} = \frac{H_1(T_0)}{H_2(T_0)} = F_{12}(T_0) \Rightarrow T_0 = F_{12}^{-1}(I_1/I_2)$$

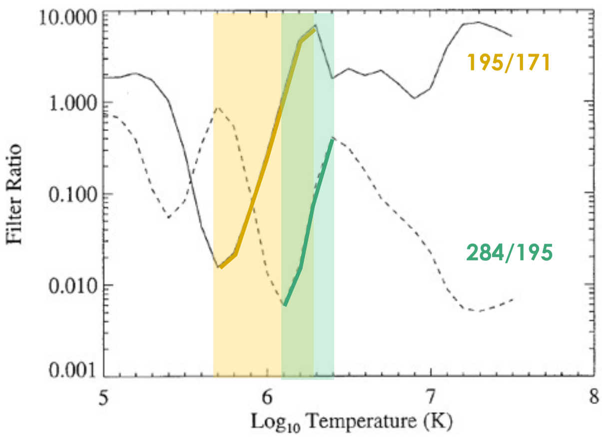

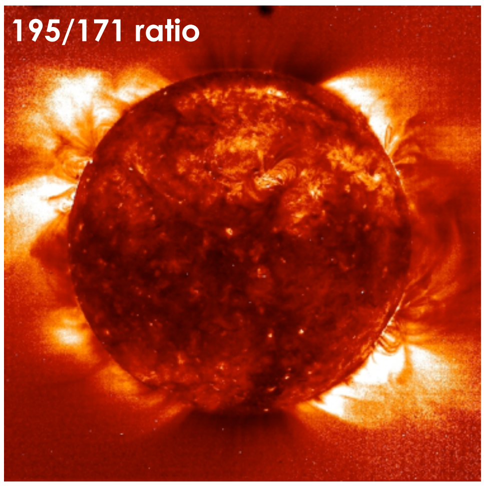

Solar Dynamics Observatory

The Atmospheric Imaging Assembly (AIA) on board SDO is the current generation of EUV imager but works on similar principles as EIT but at higher spatial and temporal resolution and with more bandpasses.

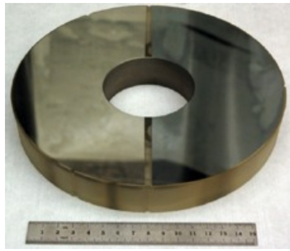

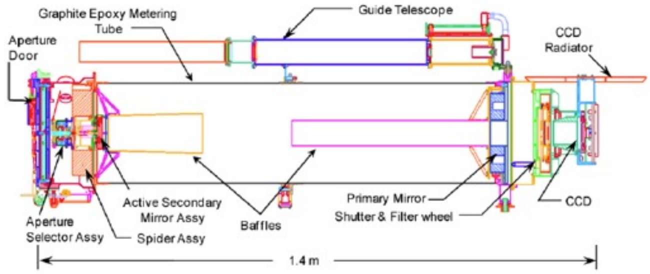

Lemen et al. (2012)

Solar Dynamics Observatory

What advantages does the SDO-era bring?

- Same spatial resolution as TRACE
- An improved time resolution but not dramatically different from TRACE

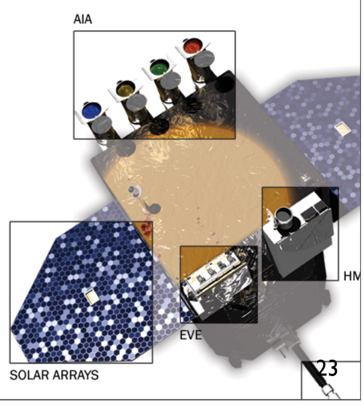

What advantages does the SDO-era bring?

- Same spatial resolution as TRACE
- An improved time resolution but not dramatically different from TRACE
- Full-sun FOV and synoptic program means no event will be missed.
- SDO/AIA can be relied upon for spectroscopic studies
- Statistical studies are now only limited by man-power!
- No SAA occurring just when it is interesting
- Multiple simultaneous bandpasses: explore phenomena beyond bulk to hot and cool coronal plasma.
- Combination with STEREO is useful for geometry estimates

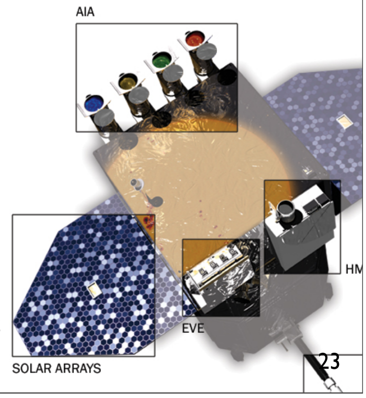

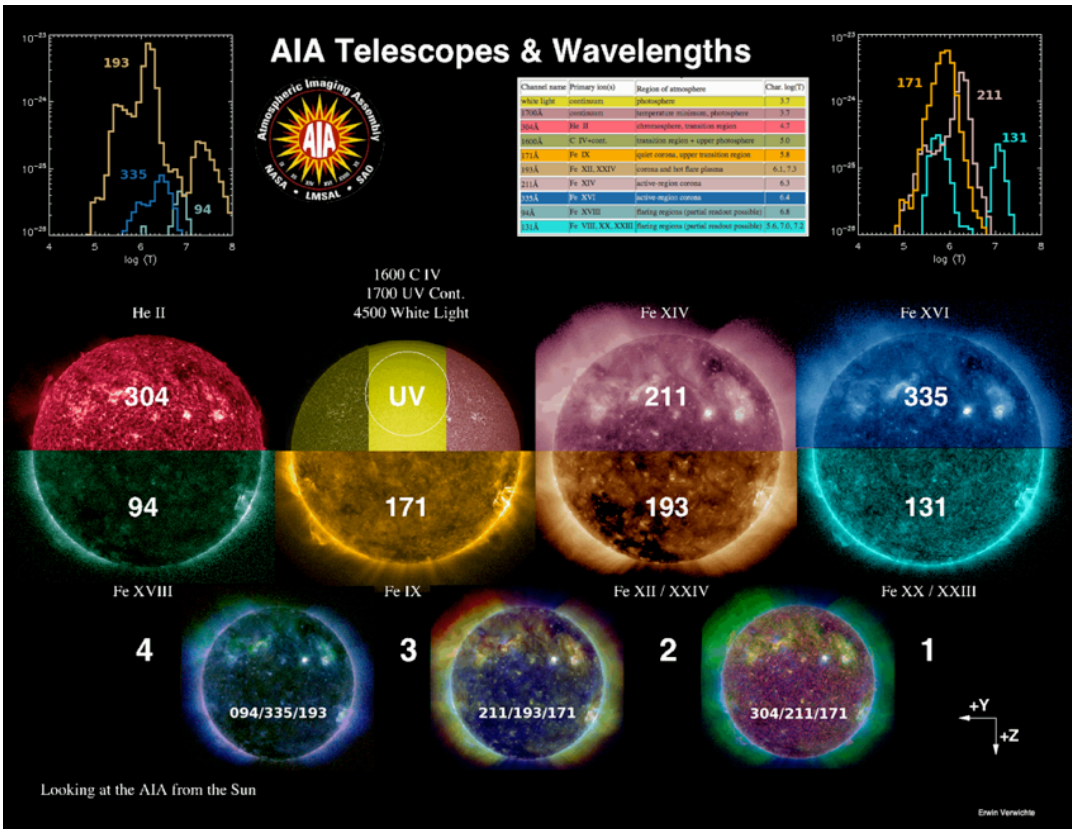

Solar Dynamics Observatory

Combining bandpasses (171,193 and 211) in three-colour channels gives an idea of temperature.

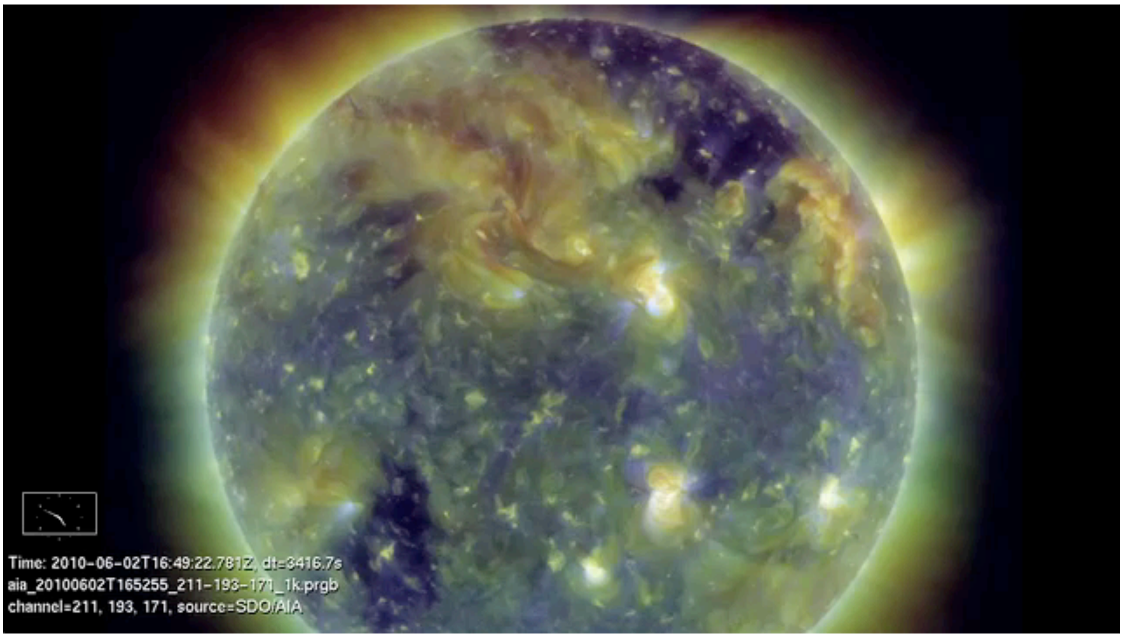

DEM method

Again, we may estimate single temperature and density in the line-of-sight.

1) We assume that DEM(T) is of the form:

$$\mathrm{DEM}(T) = \mathrm{EM}_0 \frac{1}{\sqrt{2\pi}\Delta T} \exp\left[-\frac{1}{2}\left(\frac{T-T_0}{\Delta T}\right)\right]$$

which in the limit of $\Delta T \longrightarrow 0$, becomes $\mathrm{DEM}(T) = \mathrm{EM}_0\, \delta(T-T_0)$.

2) The intensity (DN/s) of each bandpass is then of the form:

$$I_i = \mathrm{EM}_0 \int_0^\infty \frac{H_i(T)}{\sqrt{2\pi}\Delta T} \exp\left[-\frac{1}{2}\left(\frac{T-T_0}{\Delta T}\right)\right] \mathrm{d}T = \mathrm{EM}_0\, h_i(T_0, \Delta T)$$

3) For every value of T_0 and ΔT, we calculate EM_0:

$$\mathrm{EM}_0 = \frac{\sum_i I_i}{\sum_i h_i(T_0, \Delta T)}$$

4) We find the best values of T_0 and ΔT, and hence EM_0, by minimizing the difference with the observations□

$$\chi^2 = \frac{1}{n_\lambda - 2} \sum_i \left(\frac{I_i - \mathrm{EM}_0\, h_i(T_0, \Delta T)}{\sigma_{\mathrm{noise}}}\right)^2$$

DEM method

Example from Aschwanden et al. (2011)

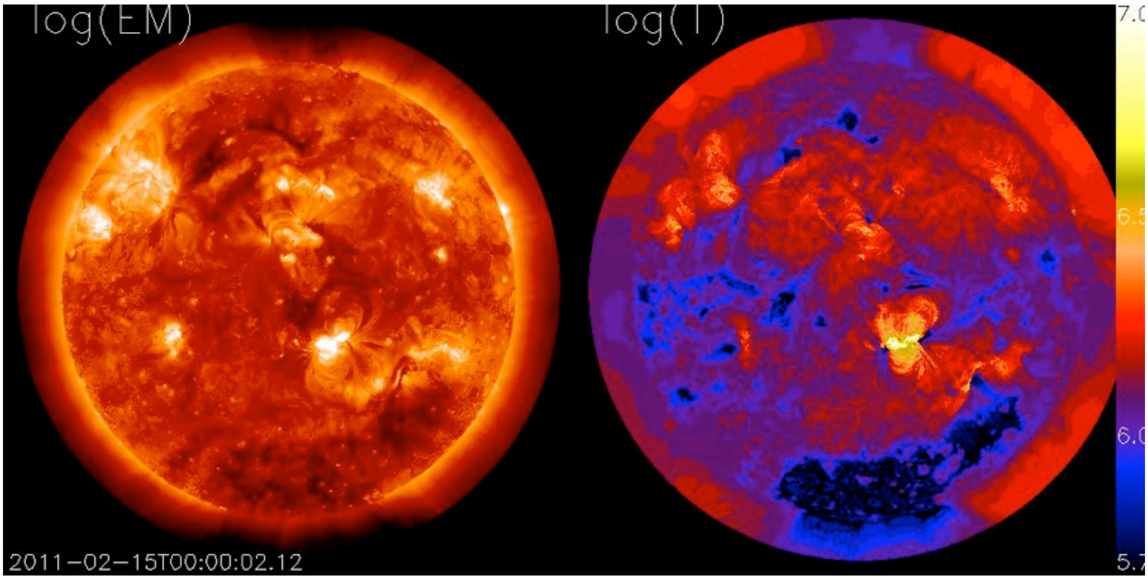

Note that this is an approximate method as the DEM(T) is highly idealised.

DEM method

More formally, you can write DEM(T) as made from many temperature bins:

$$\mathrm{DEM}(T) = \sum_j \mathrm{DEM}_j(T_j)$$

where $\mathrm{DEM}_j(T)$ are known profiles. Then the intensity (DN/s) has the form:

$$I_i = \sum_j \int_0^\infty H_i(T)\, \mathrm{DEM}_j(T_j)\, \mathrm{d}T = \sum_j H_i(T_j)\, \mathrm{DEM}_j(T_j) = \sum_j h_{ij}\, \mathrm{DEM}_j$$

The problem then becomes a matter of inverting the matrix h_{ij} to find DEM_j from I_i:

$$\mathrm{DEM}_j = \sum_i h_{ij}^{-1}\, I_i$$

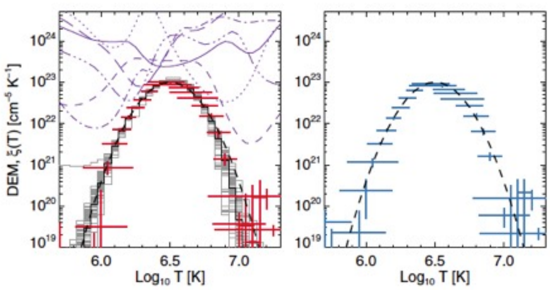

Hannah & Kontar (2012)

However, this inversion is often ill-posed as the information from a limited number of bandpasses is not enough. Careful regularization techniques then need to be employed and image noise taken into account.

Photon noise

The measured intensity is subject to errors. It is important to know about to avoid mistakes. An inherent image noise is **photon noise** (or shot noise).

The more photons collected the better resolved (crisper) the image becomes.

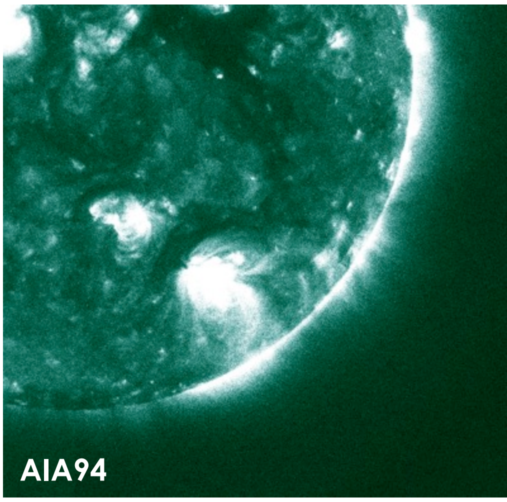

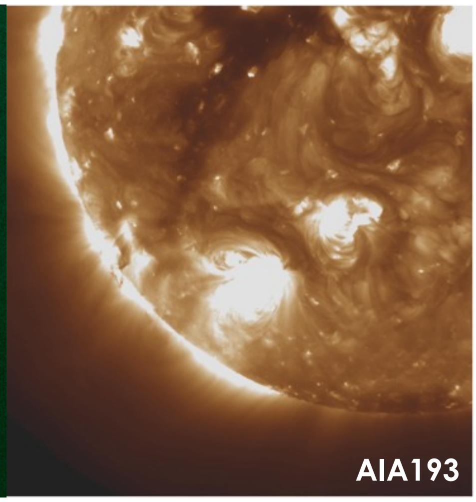

Lower signal-to-noise (fuzzier) | Higher signal-to-noise (crisper)

Photon noise

Example of constant, uniform rain on the pavement:

In the beginning, each tile will have much variation of small number of rain spots.

After much rain, the spread is practically uniform.

Photon noise

Example of constant, uniform rain on the pavement:

In the beginning, each tile will have much variation of small number of rain spots.

After much rain, the spread is practically uniform.

Photon noise

Photons hitting a CCD pixel are independent random events (similar to rain drops hitting the pavement). The distribution of the photons follows Poisson statistics (for large intensity it becomes Gaussian).

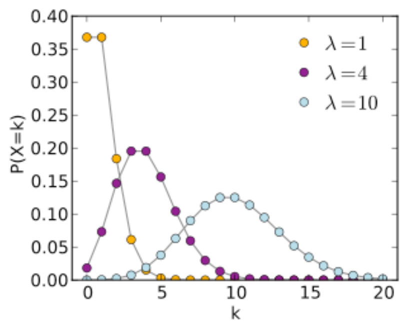

Poisson distributions as a function of number of occurrences k

The standard deviation of N photons is $\sigma = \sqrt{N}$. Relating back to the formula for image intensity, N relates to I for exposure time Δt as

$$N = \frac{I\,\Delta t}{\int G(\lambda)\,\mathrm{d}\lambda}$$

where $G(\lambda)$ is the gain [DN/photon]. The photon noise then becomes

$$\sigma^2 = \frac{I\,\Delta t}{\int G(\lambda)\,\mathrm{d}\lambda}$$

Hence the signal-to-noise ratio SNR becomes

$$\mathrm{SNR} = \frac{I\Delta t}{\sigma} = \sqrt{\int G(\lambda)\mathrm{d}\lambda}\;\sqrt{I\,\Delta t}$$

The larger the exposure time, the less effect of photon noise.

Instrumental noise

The processing of the measured light by the electronics is a source of noise.

1) Dark current noise: even if the CCD is un-exposed, the finite temperature induces spurious signals. That is why CCD are cooled. $\sigma = \sigma(T_{CCD})$.

2) Read-out noise: in a CCD the signal per pixel (photon-induced electrons) are collected in rows towards one direction.

3) Digitization noise: the signal is converted to an integer (range of power of two), this introduced an uncertainty of σ = 0.5 DN.

4) Compression noise: to save bandwidth in storing and sending images to Earth, JPEG compression is used.

5) Processing noise: e.g. de-spiking to remove cosmic-ray hits (sometimes better not to do).

$$\sigma^2 = \sigma^2_{\rm photon}(I\Delta t) + \sigma^2_{\rm dark}(T_{\rm CCD}) + \sigma^2_{\rm read} + \sigma^2_{\rm dig} + \sigma^2_{\rm comp} + \sigma^2_{\rm proc} + \ldots$$

Example: typical AIA 171Å image: $\sigma \approx \sqrt{2.3 + 0.06\, I\Delta t}$ DN

Aschwanden et al. (2000), Ding & Nakariakov (2012)

Example of cosmics

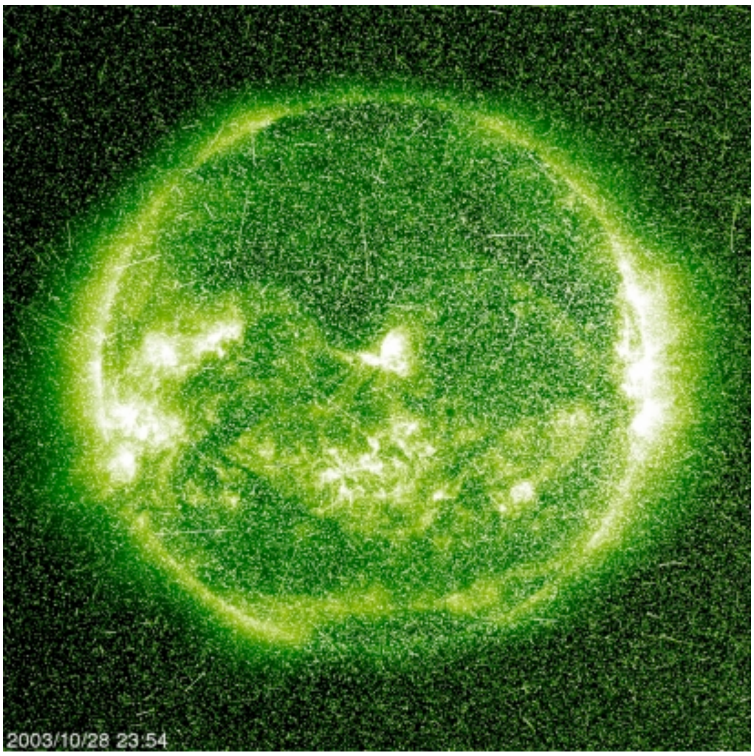

Example of an observational study

We look at an example study of using EIV imaging data:

measurement of rotation of the Sun using coronal bright points seen by EUVI on board STEREO.

Extreme UltraViolet Imager (EUVI)

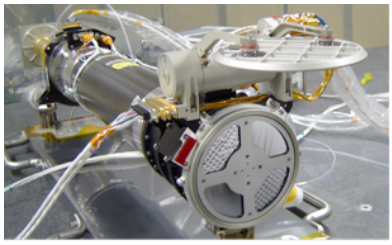

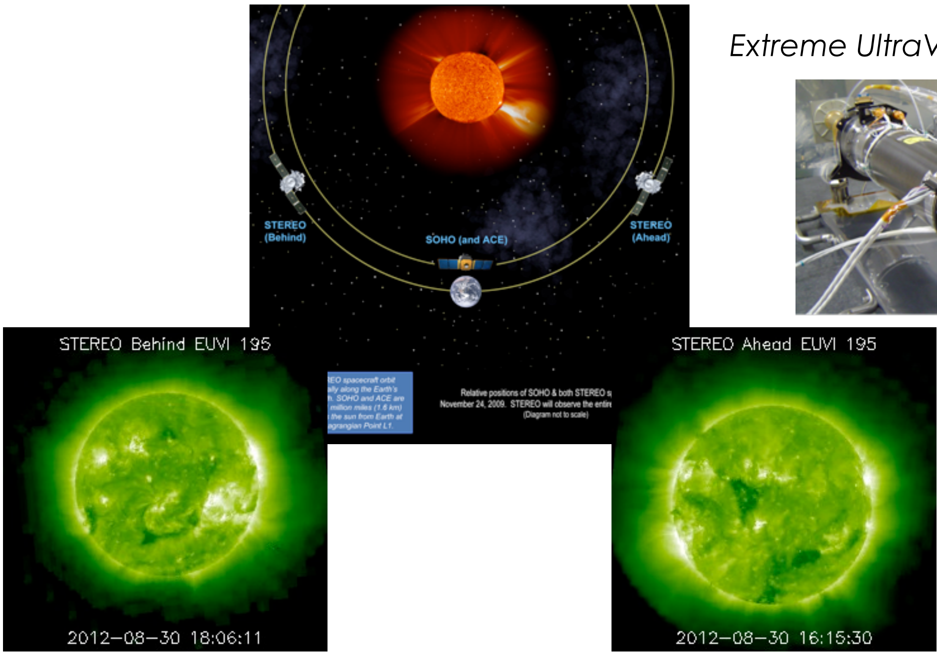

Typical data-analysis chain

Observation

Selection of the best data-set for the problem.
What temporal, spatial, spectral resolution is there?

Typical data-analysis chain

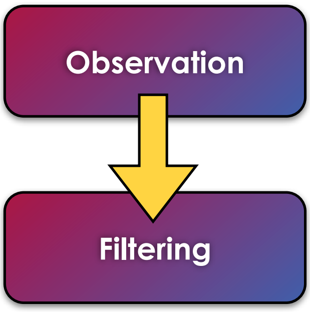

Selection of the best data-set for the problem.
What temporal, spatial, spectral resolution is there?

Enhancement of the feature or event to detect, e.g. background subtraction, running-difference, gradient filters.

Typical data-analysis chain

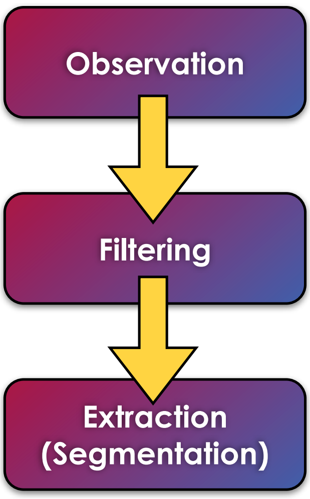

Selection of the best data-set for the problem.
What temporal, spatial, spectral resolution is there?

Enhancement of the feature or event to detect, e.g. background subtraction, running-difference, gradient filters.

Detection of the feature or event. This can be done in an automated way (objective and scaleable) or by hand (mouse-clicking and tennis arms).

Typical data-analysis chain

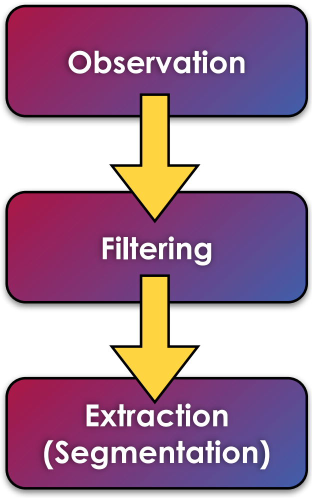

Selection of the best data-set for the problem.
What temporal, spatial, spectral resolution is there?

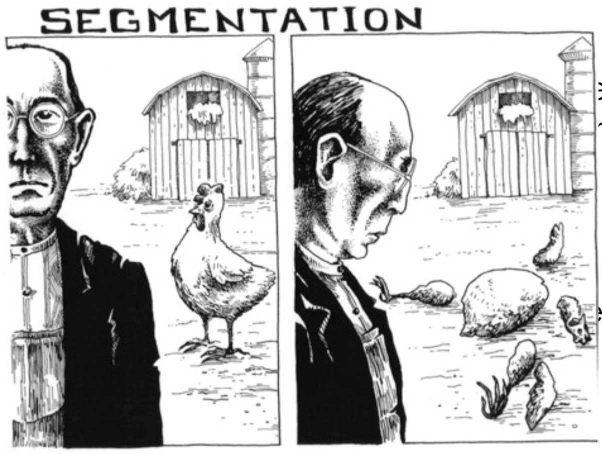

Enha etect,
e.g. k rence,
grad

Dete be done
in an eable) or
by hc

Typical data-analysis chain

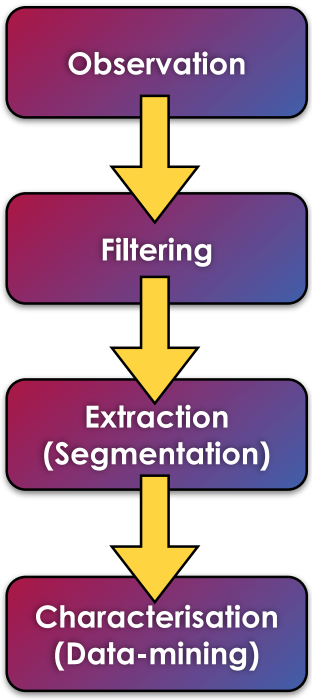

Selection of the best data-set for the problem.
What temporal, spatial, spectral resolution is there?

Enhancement of the feature or event to detect,
e.g. background subtraction, running-difference,
gradient filters.

Detection of the feature or event. This can be done
in an automated way (objective and scaleable) or
by hand (mouse-clicking and tennis arms).

Characterisation of the results: connect to physical
quantities, statistical trends and theoretical models.

Typical data-analysis chain

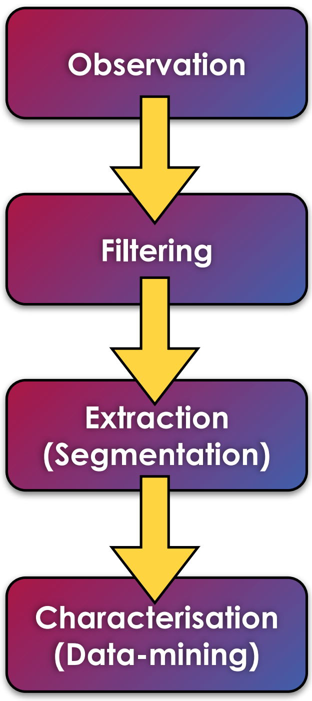

Selection of the best data-set for the problem.
Wh… there?

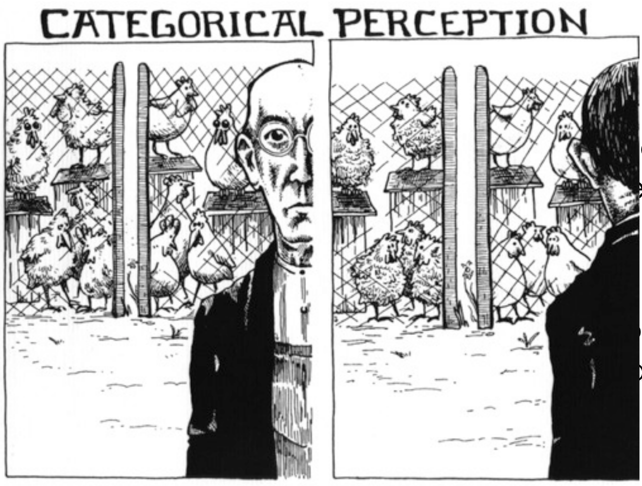

Enh… ect,
e.g. … nce,
gra…

Det… e done
in a … able) or
by …

Characterisation of the results: connect to physical quantities, statistical trends and theoretical models.

Solar rotation using bright points

We select a month worth of data from STEREO-A and STEREO-B during solar minimum when there are not many active regions and bright points are clear.

Bright points are nice local point-like features (mini active regions) that live long enough and can be used as tracers of the rotation of the Sun.

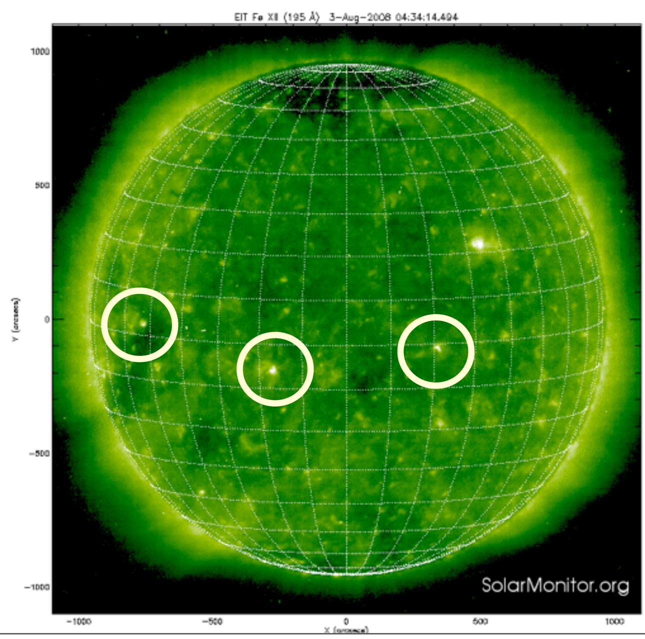

Wavelet filtering to enhance bright points

We filter the EUVI images using a two-dimensional wavelet transform:

$$\mathcal{W}_a(I)(\vec{r}) = \frac{1}{a^2} \int_{-\infty}^{+\infty} I(\vec{r}')\, \psi\left(\frac{\vec{r}' - \vec{r}}{a}\right)\, \mathrm{d}^2\vec{r}'$$

which is basically a 2d convolution of the image with Ψ(x,y), which is the mother wavelet with the special characteristic that its average is zero.

The transform enhances anything that looks like the wavelet at a certain scale *a*. Here we take the Mexican Hat wavelet, which is of the form:

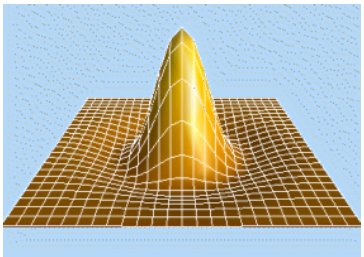

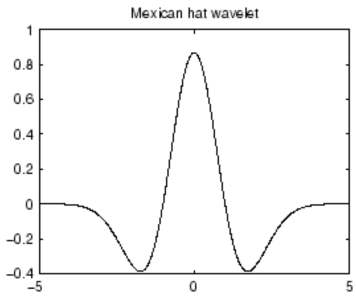

$$\psi(\vec{r}) = -\nabla^2 \exp\left(-\frac{r^2}{2}\right)$$

Wavelet filtering to enhance bright points

An original image

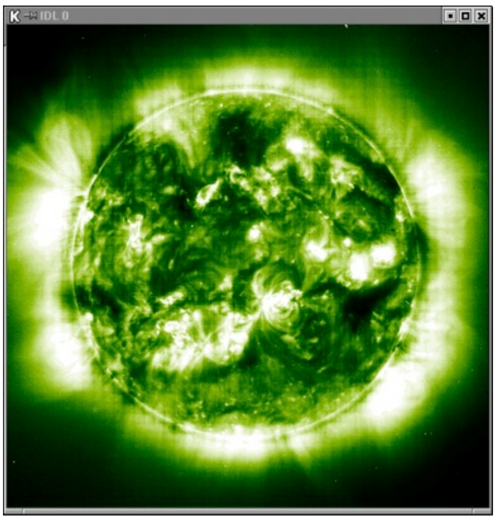

Wavelet transform at four scales

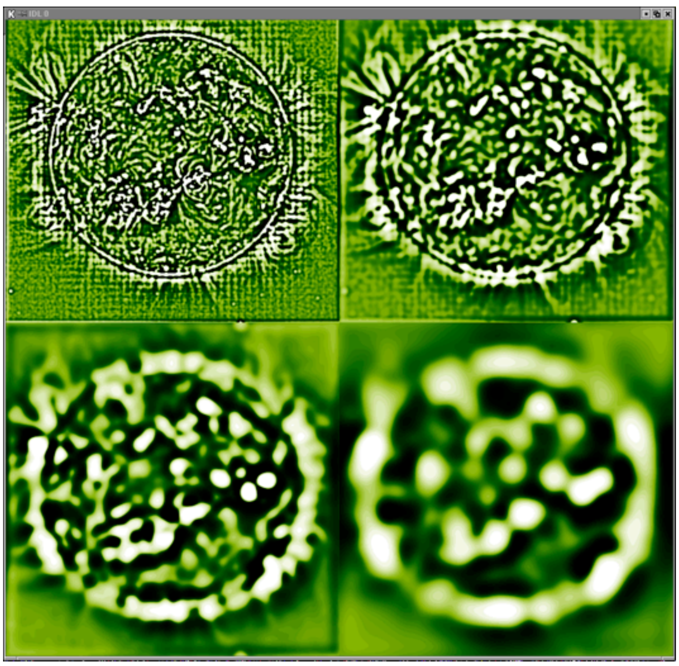

Wavelet filtering to enhance bright points

If you take the wavelet transform of a bright-point, modeled as a 2d Gaussian:

$$I(\vec{r}) \;=\; A\,\exp\left(-\frac{(\vec{r}-\vec{r}_0)^2}{2\sigma^2}\right)$$

we find the wavelet back again but with an amplitude that depends on *a*

$$\mathcal{W}_a(I)(\vec{r}) \;=\; 2\pi A\,\frac{a^2}{a^2+\sigma^2}\,\psi\left(\frac{\vec{r}-\vec{r}_0}{\sqrt{a^2+\sigma^2}}\right)$$

For $a = \sigma$ we find the maximum wavelet amplitude. So we can find the scale of the bright point easily by scanning in *a*. Also, the transform is still centered on $\boldsymbol{r}_0$, so we have no shifts (Gaussian blurring can induce such).

Also, the wavelet transform removes any background trend (as perceived at scale *a*) since the transform of the following is zero!

$$I(\vec{r}) \;=\; I_0 + ax + by$$

Detection of bright-points

Bright points average position is extracted by tresholding the wavelet transform at the optimum scale *a*. But not all detection are correct (remove cosmics)!

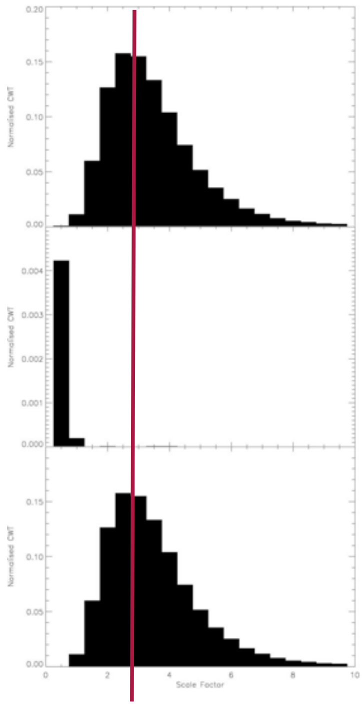

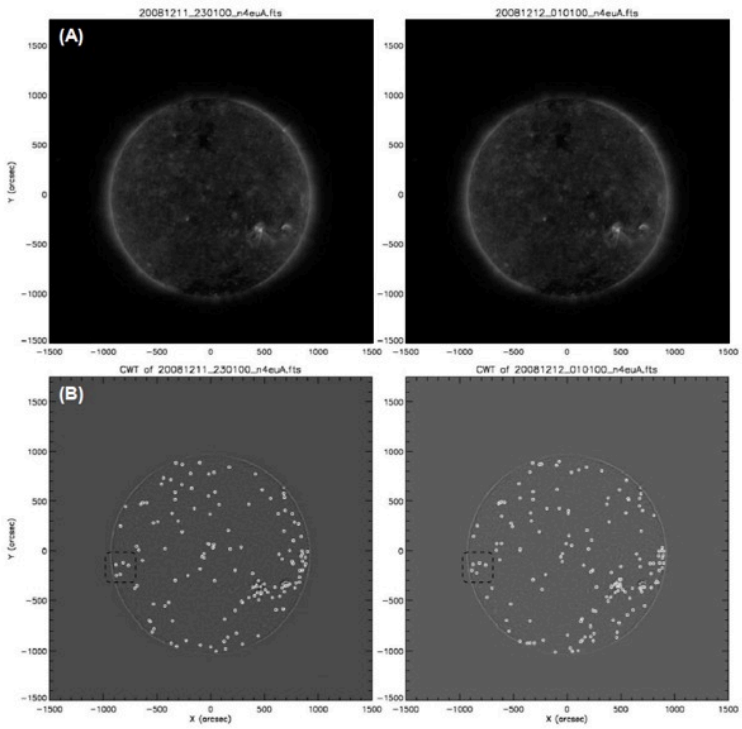

Detection of bright-points

Looking at extracted bright-points from different times, their movement on the disk, and hence their siderical rotation rate can be determined!

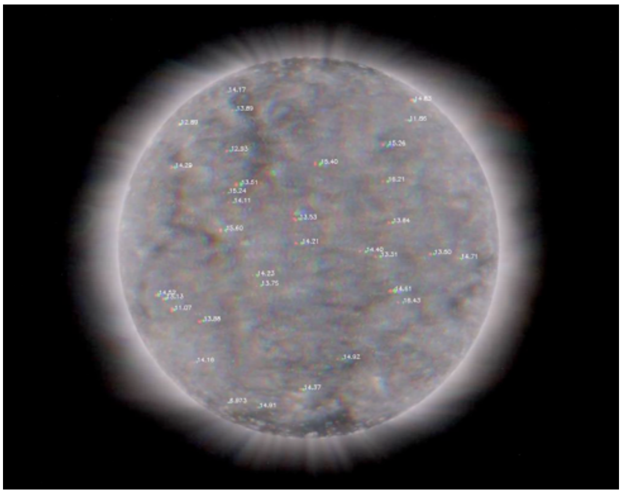

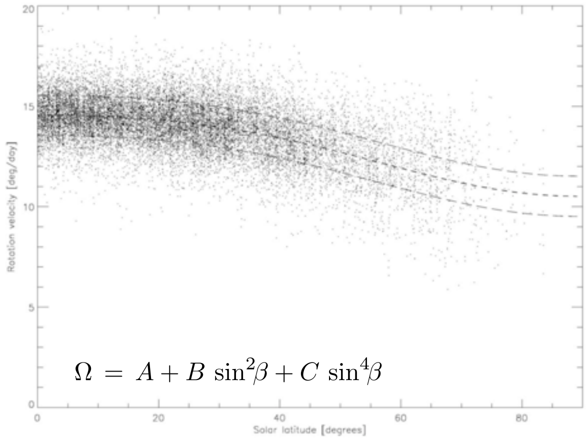

And using both STEREO's we can find the height of the bright-points in the solar atmosphere!

Bright point rotation (not height corrected)

$$\Omega = A + B\,\sin^2\beta + C\,\sin^4\beta$$

Tracer/method	$A \pm \sigma_A$	$-B \pm \sigma_B$	$-C \pm \sigma_C$	
Coronal bright points: 5	14.57 ± 0.05	2.37 ± 0.22	1.33 ± 0.52	1
Coronal bright points: 6(a)	14.63 ± 0.06	3.01 ± 0.22		2
Coronal bright points: 6(b)	14.69 ± 0.23	2.94 ± 1.12		3
Coronal bright points	14.65 ± 0.2			[21]
Coronal bright points	14.6 ± 0.3			[22]
Coronal bright points	14.530 ± 0.032	2.68 ± 0.13		[23]
Coronal bright points	14.677 ± 0.033	3.10 ± 0.14		[23]
Sunspots	14.522 ± 0.004	2.84 ± 0.04		[24]
Sunspots	14.393 ± 0.010	2.95 ± 0.09		[24]
Sunspots	14.551 ± 0.006	2.87 ± 0.06		[25]
Sunspots	14.531 ± 0.003	2.75 ± 0.05		[26]
Sunspots	14.37 ± 0.01	2.59 ± 0.16		[27]
Hα filaments	14.48	2.16		[29]
Hα filaments	14.45	1.43		[30]
Hα filaments	14.45 ± 0.15	0.11 ± 0.90	3.69 ± 0.90	[31]
Coronal bright points	14.495 ± 0.026	1.89 ± 0.06	1.89 ± 0.06	[23]
Coronal bright points	14.454 ± 0.027	2.22 ± 0.07	2.22 ± 0.07	[23]
Magnetic	14.307 ± 0.005	1.98 ± 0.06	2.15 ± 0.11	[32]
Magnetic	14.42 ± 0.02	2.00 ± 0.13	2.09 ± 0.15	[33]
Magnetic	14.00 ± 0.54	2.24 ± 1.22	1.78 ± 0.79	[34]
Doppler	13.76	1.74	2.19	[35]
Doppler	14.05	1.49	2.61	[36]
Doppler	13.99 ± 0.06			[37]
Doppler	13.92 ± 0.12			[38]

[1] Results from present report [tracing method].
[2] Results from present report [mathematical imaging method (a)]
[3] Results from present report [mathematical imaging method (b)]

Another example of observational study

We consider an observation by STEREO/EUVI of a transverse loop oscillation on 26/06/2007 from two vantage points [Verwichte et al. 2009].

EUVI properties
- Full disk images (304Å, 171Å, 195Å, 284Å)
- 1.6 arcsec CCD pixel size
- Time cadence of 2.5 minutes

A 10 min oscillation is visible in the southern loop arcade of an active region on the East limb.

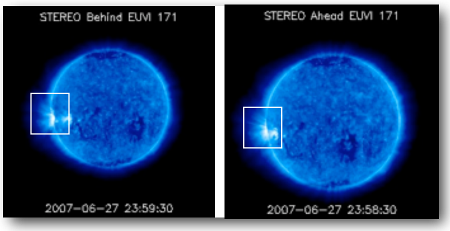

42
Erwin Verwichte - Sun Observation - ASSSP12

Another example of observational study

We consider an observation by STEREO/EUVI of a transverse loop oscillation on 26/06/2007 from two vantage points [Verwichte et al. 2009].

EUVI properties
- Full disk images (304Å, 171Å, 195Å, 284Å)
- 1.6 arcsec CCD pixel size
- Time cadence of 2.5 minutes

A 10 min oscillation is visible in the southern loop arcade of an active region on the East limb.

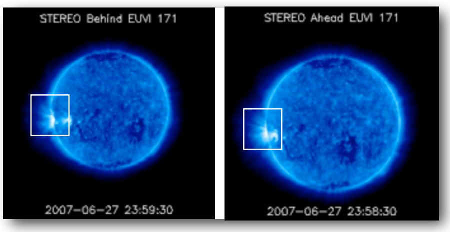

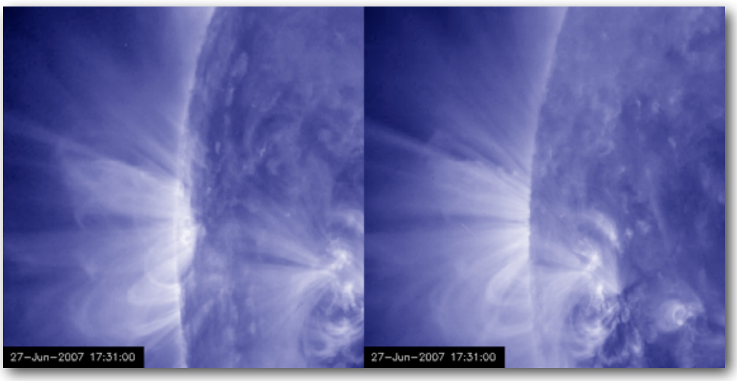

Another example of observational study

With the geometry known we compare simulated oscillations for various polarisations and harmonics with the data.

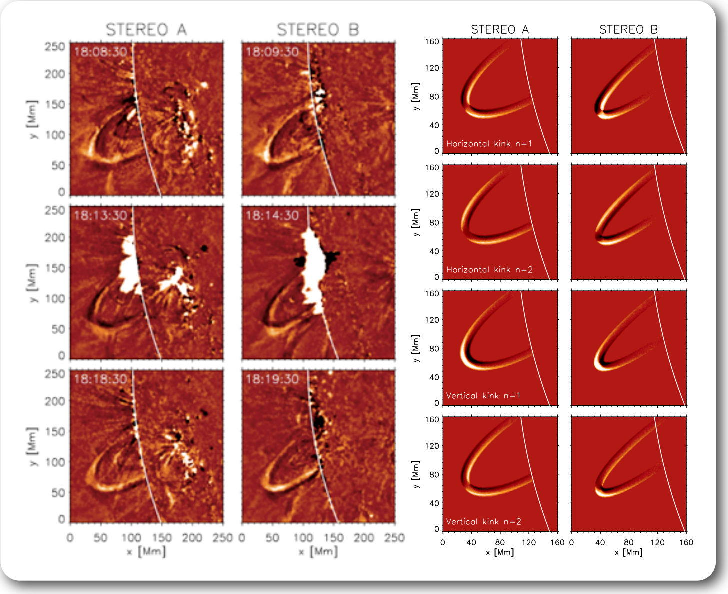

Suggests observed mode is horizontally polarised fundamental kink mode.

42
Erwin Verwichte - Sun Observation - ASSSP12

Another example of observational study

With the geometry known we compare simulated oscillations for various polarisations and harmonics with the data.

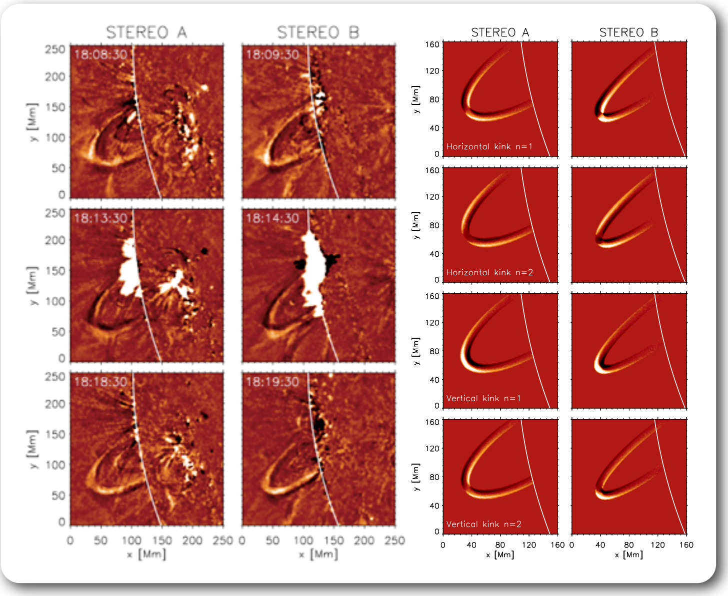

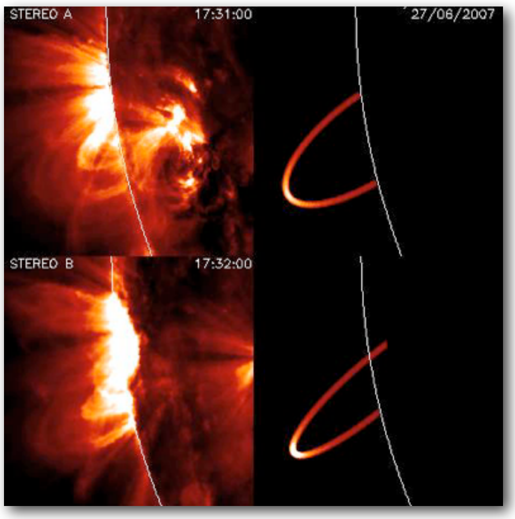

Suggests observed mode is horizontally polarised fundamental kink mode.

Stereoscopy

Stereoscopy means using two view points to reconstruct a 3d picture of a structure if the angle between the views is not too large.

This does not give a unique solution as we need 3 non co-planar views to have all information. So with STEREO it works well except when structures (such as loop) are oriented in the epipolar plane of STEREO-A, B and Sun.

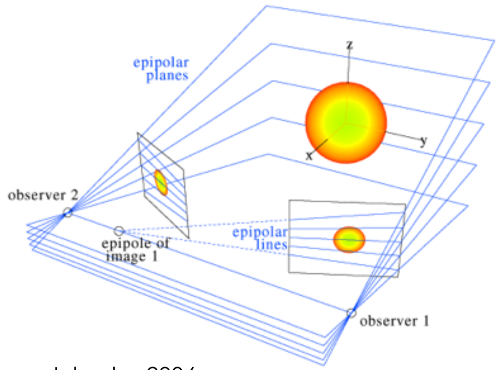

Inhester 2006

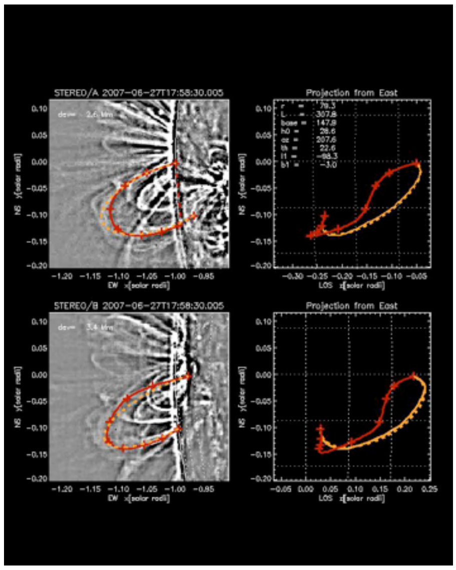

Aschwanden, 2009

Stereoscopy

One may add a model to aid 3d reconstruction. For instance one may assume that a loop is planar (all points in the same plane). Then one adjusts the inclination of the loop plane to find the best match between the two views. This works well for large separation angles between views, but is always approximate.

This can be done between two instantaneous views (e.g. STEREO-AIA) or between two times (dynamic stereoscopy).

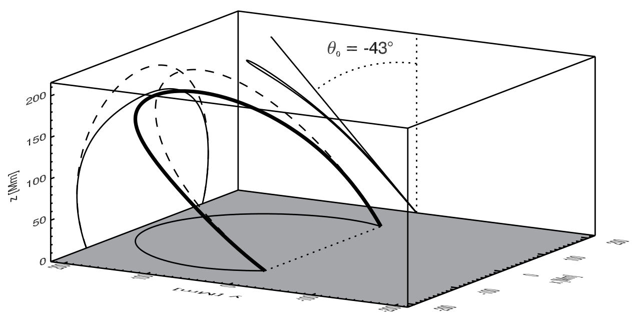

Verwichte et al. 2009, 2010

Another example of observational study

The full sun, high-cadence synoptic, multi-wavelength view from AIA/SDO provides rich pickings in oscillation events (>200 events!).
The combination with STEREO allows for a good estimate of 3d structure.

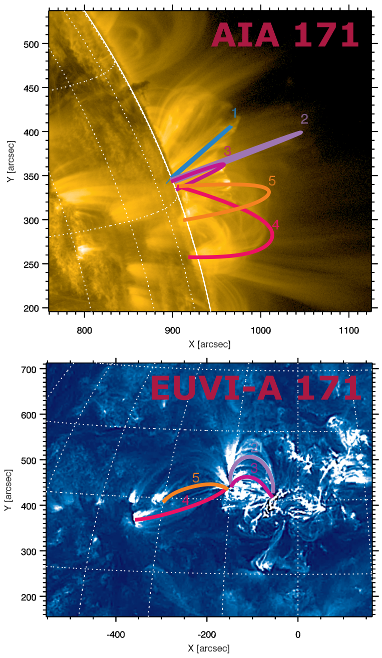

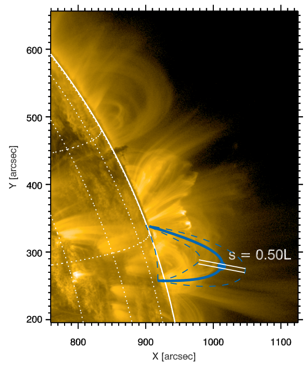

~90° view separation with STEREO is useful!

Example of a vertical TLO